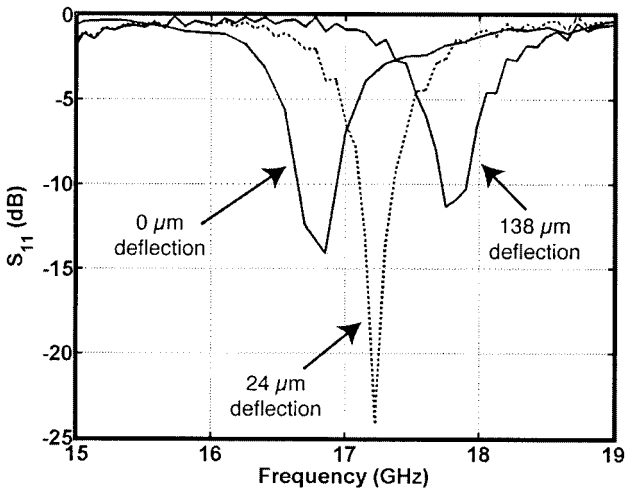

Figure 8 Measured S_{11} parameters for the 18.9-GHz MPA at three different ground-plane deflections

The measured results, however, are seen to perform better than the simulated ones for deflections from 22 to 100 μm. This discrepancy may possibly be due to the membrane possessing a nonuniform deflection as it is pulled down. In our deflection measurements, the membrane deflection was measured at the membrane centre. However, for our corrugated membrane, it is possible that the membrane possessed a greater deflection slightly off centre. If this was the case, then our measured deflection at the membrane centre would be less than the average deflection over the entire membrane surface, which would explain the performance discrepancy between the two curves in Figure 9. Nevertheless, the agreement is surprisingly close.

5. CONCLUSION

A frequency-tunable MPA has been fabricated using a micromachined reconfigurable ground-plane membrane. Electrostatic actuation of the membrane away from the antenna-patch substrate introduced a controllable air-gap thickness between the substrate and the copper ground plane. The resonant frequency of the MPA was controllable between 16.8 and 17.82 GHz for a ground-plane deflection from 0 to 138 μm. This represents an approximately 6% controlled variation in the resonant frequency of the MPA. These measured results are in close agreement with the simulated performance of the MPA using Ensemble 8.0.

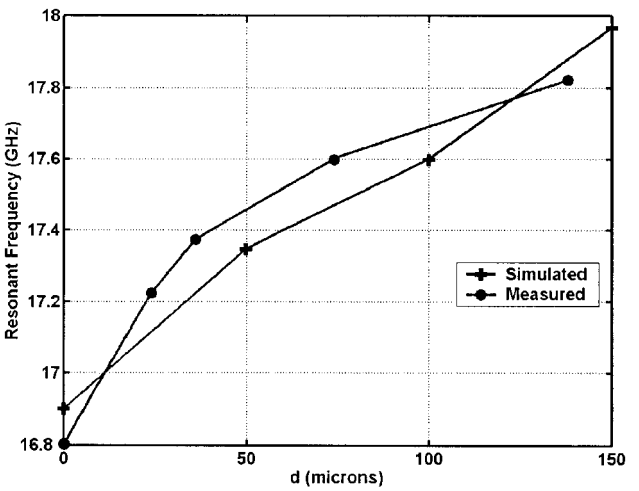

Figure 9 Comparison of the 18.9-GHz MPA's Ensemble-simulated and VNA-measured resonant frequencies for varying air-gap heights

ACKNOWLEDGMENTS

This research was funded by the Natural Sciences and Engineering Research Council (NSERC) of Canada and the Canadian Institute of Telecommunication Research (CITR).

REFERENCES

1. J.-C. Chiao, Y. Fu, I.M. Chio, M. DeLisio, and L.-Y. Lin, MEMS Reconfigurable Vee Antenna, IEEE MTT-S Int Microwave Symp Dig 4 (1999), 1515–1518.
2. R.N. Simons, D. Chun, and L.P.B. Katehi, Microelectromechanical systems (MEMS) actuators for antenna reconfigurability, IEEE MTT-S Int Microwave Symp Dig 1 (2001), 215–218.
3. W.H. Weedon, W.J. Payne, and G.M. Rebeiz, MEMS-switched reconfigurable antennas, IEEE AP-S Int Symp Dig 3 (2001), 654–657.
4. J.S. Dahele and K.F. Lee, Theory and experiment on microstrip antennas with air-gaps, IEEE Proc 132 (1985).
5. J.-C. Langer, J. Zou, and C. Liu, Micromachined reconfigurable out-of-plane microstrip patch antenna using plastic deformation magnetic actuation, IEEE Microwave Wireless Compon Lett 13 (2003), 120–122.
6. C. Shafai, S.K. Sharma, and L. Shafai, Microstrip phase shifter using actuating ground plane membrane, ANTEM 2002 Symp Antenna Technol and Appl Electromagn Montréal, Canada, 2002, pp. 592–595.

DC TO 6-GHz HIGH-GAIN LOW-NOISE GaInP/GaAs HBT DIRECT-COUPLED AMPLIFIERS WITH AND WITHOUT EMITTER-CAPACITIVE PEAKING

C. C. Meng,[1] T. H. Wu,[1] and S. S. Lu[2]
[1] Department of Communications Engineering
National Chiao Tung University
Taiwan, R.O.C.
[2] Department of Electrical Engineering
National Taiwan University
Taiwan, R.O.C.

Received 11 March 2004

ABSTRACT: *High-gain shunt-series shunt-shunt wideband amplifiers with and without emitter-peaking capacitors are demonstrated by using GaInP/GaAs HBT technology. Experimental results show that the power gain is 28 dB from DC to 6 GHz for a wideband amplifier without emitter-peaking capacitors. On the other hand, a wideband amplifier with emitter-peaking capacitors can increase the gain bandwidth up to 8 GHz at the cost of lower input/output return loss. Both circuits have similar power and noise performance. The noise figures of both designs are less than 2.8 dB for frequencies below 6 GHz. OP_{1dB} and OIP_3 are 7 and 20 dBm at 2 GHz, respectively. Total current consumption is 67 mA at 5-V supply voltage for both wideband amplifiers.* © 2004 Wiley Periodicals, Inc. Microwave Opt Technol Lett 43: 67–69, 2004; Published online in Wiley InterScience (www.interscience.wiley.com). DOI 10.1002/mop.20377

Key words: *GaInP; HBT; amplifier*

1. INTRODUCTION

Wideband amplifiers [1–4] play an important role in modern wireless-communication systems. The essential design approach of a wideband amplifier is dual-feedback-loop technology. A dual-

feedback-loop configuration (shunt-series shunt-shunt) is used to achieve matched-impedance wideband amplifiers in this paper. The circuit schematic of the designed shunt-series shunt-shunt GaInP/GaAs HBT wideband amplifier is illustrated in Figure 1. Resistors R_{f1} and R_{f2} in Figure 1 are the global-feedback and local-feedback resistors, respectively. A Darlington pair is used in the second stage to improve the frequency response. A shunt-series shunt-shunt amplifier has intrinsic over-damped characteristics in gain response under matched-impedance conditions; thus, an emitter-capacitive gain-peaking technique is used to extend the power-gain bandwidth by compensating the intrinsic over-damped frequency response of power gain [2, 5]. In this paper, two nearly identical wideband amplifiers (one with emitter-peaking capacitors and the other without emitter-peaking capacitors) are fabricated in order to compare the performances. C_{e1} and C_{e2} are the emitter-peaking capacitors, as shown in Figure 1.

2. PRINCIPLES OF CIRCUIT DESIGN

A photograph of the fabricated GaInP/GaAs HBT wideband feedback amplifiers is shown in Figure 2. There are two designs in the die. The wideband feedback amplifiers in Figure 2 were implemented using 1.4-μm emitter-width GaInP/GaAs HBT technology. The top one is a wideband amplifier with emitter-peaking capacitors and the bottom one is a wideband amplifier without emitter-peaking capacitors. The bottom device layout has been rotated 180° with respect to the top one in order to facilitate on-wafer probing. Both designs have identical transistor sizes for comparison purposes. The size of transistor Q_1 is $1.4 \times 9 \times 2$ μm, the size of transistor Q_2 is $1.4 \times 6 \times 1$ μm, and the size of transistor Q_3 is $1.4 \times 9 \times 5$ μm. The die size is 1×1 mm. Most of the die area is not fully utilized in order to facilitate the on-wafer measurement, and the die size of each wideband feedback amplifier can be easily compacted into 0.4×0.4 mm.

3. MEASUREMENT RESULTS AND DISCUSSIONS

Total current consumption is 67 mA at 5-V supply voltage for both GaInP/GaAs HBT wideband amplifiers. The first stage consumes 17 mA, whereas the second stage consumes 50 mA. The forward-transmission gain and input-return loss are illustrated in Figure 3, while the reverse-transmission gain and output-return loss are illustrated in Figure 4. The circuit without gain-peaking capacitors has 6-GHz 3-dB gain bandwidth, and S_{11} is below -15 dB and S_{22} is below -12 dB for the measurement range from DC to 18 GHz, as illustrated in Figures 3 and 4, respectively. The circuit with emitter-peaking capacitors has a higher gain bandwidth, but suffers from lower input/output return losses for frequencies above 4 GHz when gain peaking starts to appear. Thus, S_{11} reaches -8 dB, while S_{22} reaches -9 dB at 8 GHz for the circuit with emitter-peaking capacitors. In other words, some trade-offs exist between power-gain bandwidth and matched-impedance bandwidth when the emitter-peaking capacitors are introduced. Figure 5 illustrates Z_T (50Ω load transimpedance) and Z_{21} (open load transimpedance) for both designs calculated from the measured S parameters. Z_T is defined as the transimpedance gain with 50Ω load and is calculated according to the following widely used formula:

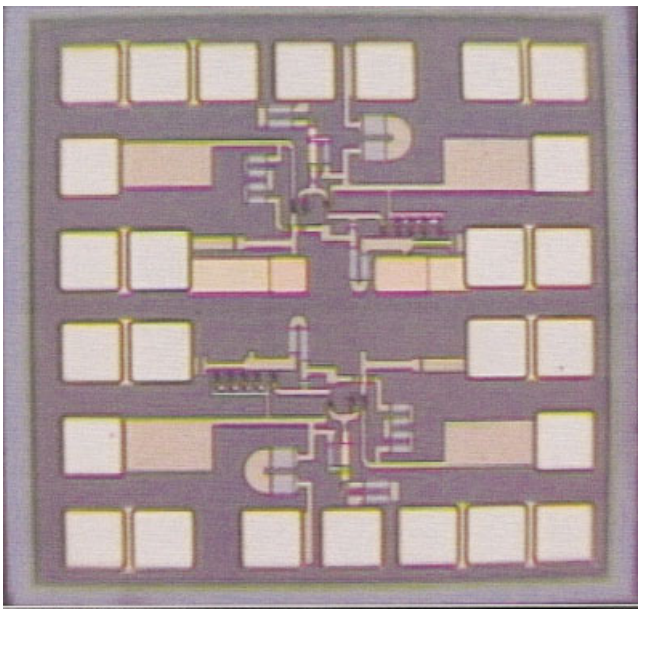

Figure 2 Die photograph of shunt-series shunt-shunt GaInP/GaAs HBT wideband amplifiers with (upper) and without (lower) emitter peaking. [Color figure can be viewed in the online issue, which is available at www.interscience.wiley.com.]

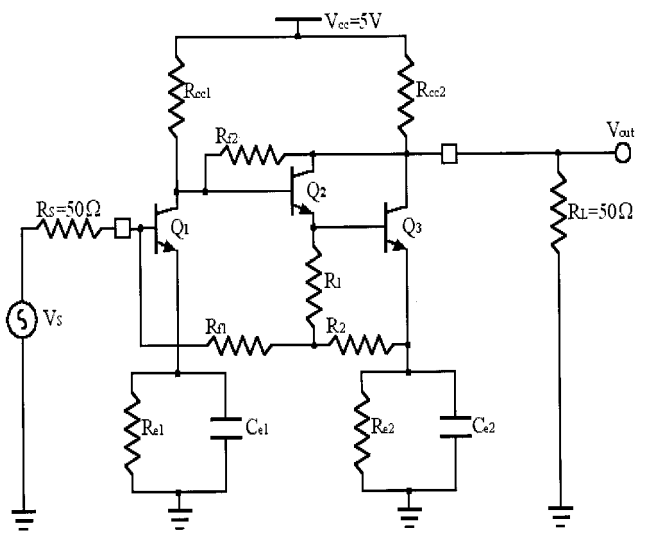

Figure 1 Circuit Schematic of a shunt-series shunt-shunt GaInP/GaAs HBT wideband feedback amplifier. C_{e1} and C_{e2} are the emitter-peaking capacitors

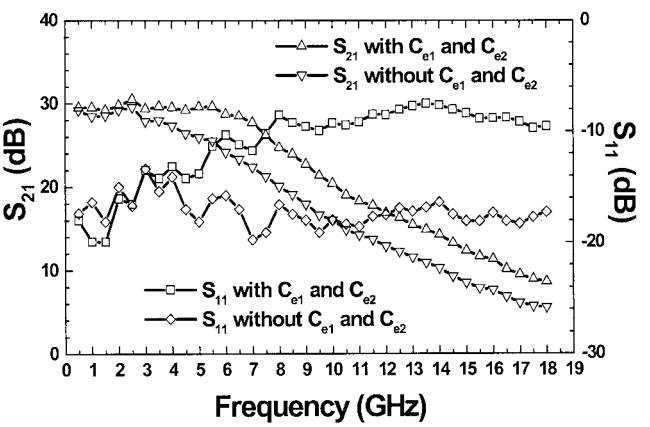

Figure 3 Measurement results of forward-transmission gain and input-return loss for GaInP/GaAs HBT wideband amplifiers with and without emitter peaking

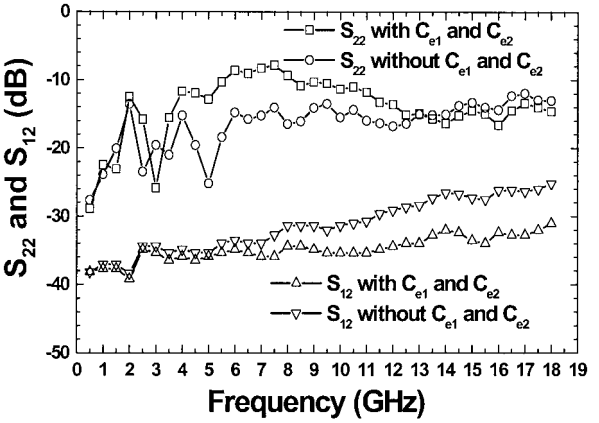

Figure 4 Measurement results of reverse-transmission gain and output-return loss for GaInP/GaAs HBT wideband amplifiers with and without emitter peaking

$$Z_T = \frac{S_{21}}{1 - S_{11}} \cdot 50.$$

The circuit using emitter-gain-peaking capacitors has 65-dBΩ gain and 8-GHz 3-dB bandwidth for Z_T, but the circuit without emitter-peaking capacitors has the same gain with 4-GHz 3-dB bandwidth for Z_T. The Z_{21} data in Figure 5 also shows that the emitter-peaking capacitors have an influence upon the Z_{21} response. Figure 6 illustrates the noise and power performances of both circuits. Both designs have similar noise figures, which are less than 2.8 dB for frequencies below 6 GHz. OP_{1dB} and OIP_3 of both circuits as functions of frequency are also illustrated in Figure 6. OP_{1dB} and OIP_3 are 7 and 20 dBm at 2 GHz, respectively. Both OP_{1dB} and OIP_3 decrease when the frequency increases. There is no apparent power-performance difference between the two designs.

4. CONCLUSION

In this paper, 28-dB gain, DC to 6-GHz GaInP/GaAs shunt-series shunt-shunt feedback wideband amplifiers have been demonstrated. The experimental results show that power gain is 28 dB and input/output return loss is below 12 dB from DC to 6 GHz for the wideband amplifier without emitter-capacitive peaking. An emitter-capacitive peaking technique can extend the 3-dB power-gain bandwidth at the cost of lower input/output return loss. The

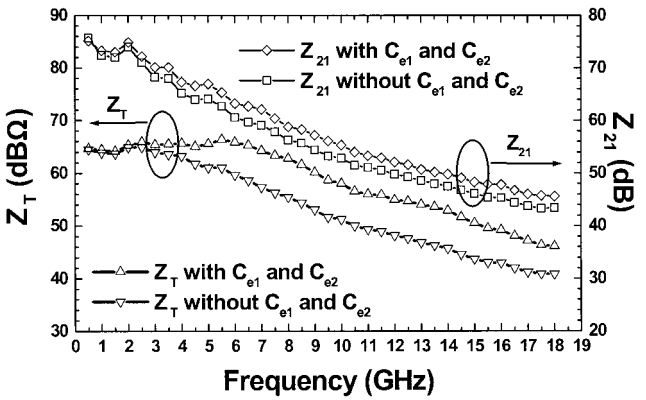

Figure 5 Measured Z_T and Z_{21} of GaInP/GaAs HBT wideband amplifiers with and without emitter peaking

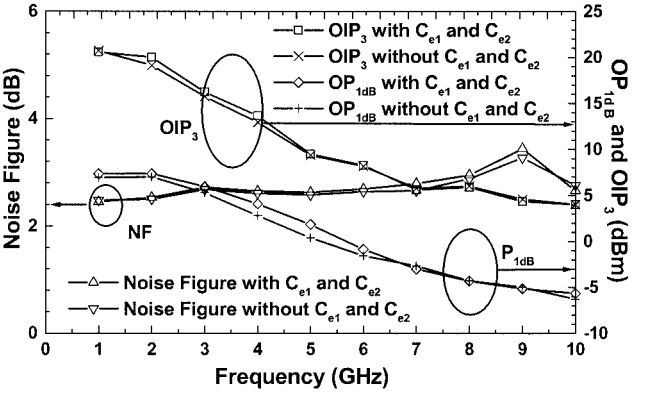

Figure 6 Measured noise figures and power performances of GaInP/GaAs HBT wideband amplifiers with and without emitter peaking

circuit using peaking capacitors has 8-GHz 3-dB power-gain bandwidth, while S_{11} reaches −8 dB and S_{22} reaches −9 dB at 8 GHz. Both circuits have similar noise and power performances. The noise figures of both circuits are less than 2.8 dB for frequencies below 6 GHz.

ACKNOWLEDGMENTS

This work was supported by the National Science Council of Republic of China under grant no. NSC 92-2219-E-009-023 and by the Ministry of Education under grant no. 89-E-FA06-2-4.

REFERENCES

1. R.G. Meyer and R.A. Blauschild, A 4-Term wide-band monolithic amplifier, IEEE J Solid State Circ SC-16 (1981), 634–638.
2. C.D. Hull and R.G. Meyer, Principles of monolithic wideband feedback amplifier design, J High-Speed Electron 3 (1992), 53–93.
3. K.W. Kobayashi and A.K. Oki, A DC-10 GHz high gain-low noise GaAs HBT direct-coupled amplifier, IEEE Microwave Guided Wave Lett 5 (1995).
4. K.W. Kobayashi and A.K. Oki, A low-noise baseband 5-GHz direct-coupled HBT amplifier with common-base active input match, IEEE Microwave Guided Wave Lett 4 (1994).
5. M.C. Chiang, S.S. Lu, C.C. Meng, S.A. Yu, S.C. Yang, and Y.J. Chan, Analysis, design, and optimization of InGaP-GaAs HBT matched-impedance wideband amplifiers with multiple feedback loops, IEEE J Solid States Circ 37 (2002), 694–701.

TENSOR PRODUCT DERIVATIVE MATCHING FOR WAVE PROPAGATION IN INHOMOGENEOUS MEDIA

Shan Zhao[1] and G. W. Wei[1,2]
[1] Department of Mathematics
Michigan State University
East Lansing, MI 48824
[2] Department of Electrical and Computer Engineering
Michigan State University
East Lansing, MI 48824

Received 10 March 2004

ABSTRACT: *We propose a tensor product derivative matching (TPDM) method to restore the accuracy of high-order finite difference time-domain (FDTD) schemes of computational electromagnetics (CEM)*